Chinese Chemical Letters 34 (2023) 107536

Contents lists available at ScienceDirect

Chinese Chemical Letters

journal homepage: www.elsevier.com/locate/cclet

A photo-elutable and template-free isothermal amplification strategy for sensitive fluorescence detection of 5-formylcytosine in genomic DNA

Hongling Yang[a], Yanfei Zhang[a], Zhenning Yu[a], Si-Yang Liu[b], Yuzhi Xu[c,*], Zong Dai[b,*], Xiaoyong Zou[a,*]

[a] School of Chemistry, Sun Yat-sen University, Guangzhou 510275, China
[b] Guangdong Provincial Key Laboratory of Sensing Technology and Biomedical Instrument, School of Biomedical Engineering, Sun Yat-sen University, Shenzhen 518107, China
[c] Scientific Research Center, The Seventh Affiliated Hospital, Sun Yat-sen University, Shenzhen 518107, China

ARTICLE INFO

Article history:
Received 22 March 2022
Revised 3 May 2022
Accepted 14 May 2022
Available online 19 May 2022

Keywords:
5-Formylcytosine
DNA demethylation
Fluorescence detection
Isothermal amplification
Magnetic separation

ABSTRACT

5-Formylcytosine (5fC), as an important epigenetic modification, plays a vital role in diverse biological processes and multiple diseases by regulating gene expression. Owing to the extremely low abundance of 5fC in all mammalian tissues and high structural similarity with other cytosine derivatives, the precise and sensitive detection of 5fC is challenging. Herein, a photo-elutable and template-free isothermal amplification strategy has been proposed for the sensitive detection of 5fC in genomic DNA based on 5fC-specific biotinylation, enrichment, photocleavage, and terminal deoxynucleotidyl transferase (TdT)-assisted fluorescence signal amplification, which is termed 5fC-PTIAS. By introducing the highly specific chemolabeling and the one-step photoelution processes, this strategy possesses a minimal nonspecific background as well as a much higher amplification efficiency. With the high signal-to-noise ratio, this strategy can achieve the accurate quantification of 5fC in various biological samples including mouse brain, kidney, and liver, with a limit of detection (LOD) of 0.025‰ in DNA (S/N = 3). These results not only confirm the widespread distribution of 5fC but also indicate its significant variation in different tissues and ages. The bisulfite- and mass spectrometry-free strategy is highly sensitive, selective, and easily mastered, holding great promise in detecting other epigenetic modifications with much lower levels.

As an endogenous oxidation intermediate in the DNA demethylation process mediated by ten-eleven translocation (TET) family proteins [1–3], 5-formylcytosine (5fC), plays an important role in a wide variety of biological processes such as cell differentiation, DNA replication, transcription, repair and recombination [4–6]. Although 5fC is an oxidation product of 5-methylcytosine (5mC), it shows great distinction in genome-wide distributions and protein affinities, indicating that they may perform different functions in epigenetic signaling [7–9]. The content of 5fC differs in tissues or cells, and even within the same specific gene, its global level also changes over time. Moreover, aberrant 5fC levels in genomes are usually associated with various cancers and poor prognosis [10,11]. Hence, accurate quantification of 5fC levels in genome is of great theoretical significance and research value for thoroughly understanding the biological function of 5fC. Nevertheless, the abundance of 5fC in human genome is extremely low, accounting for about 0.02% to 0.002% of all cytosine species, which is roughly 10- to 100-fold lower than that of 5-hydroxymethylcytosine (5hmC) [12]. Besides the extremely low abundance, 5fC has highly similar structure with other cytosine derivatives, leading to the challenge and difficulty of accurate 5fC detection.

Bisulfite-based sequencing technology has been the gold standard for the detection of 5fC with single-base resolution, but it causes severe DNA degradation due to the harsh bisulfite treatment and requires expensive and complex sequencers [13–15]. Alternatively, some other representative methods have been developed, such as liquid chromatography coupled with mass spectrometry (LC-MS/MS) and antibody-based immunoassay [16,17]. Although 5fC can be efficiently discriminated from other cytosine derivatives, the LC-MS/MS methods need sophisticated instruments and skilled operators, and the immunoassay suffers from the CpG-density-related bias of antibody and potential contaminants of

* Corresponding authors.
E-mail addresses: xuyzh28@mail.sysu.edu.cn (Y. Xu), daizong@mail.sysu.edu.cn (Z. Dai), ceszxy@mail.sysu.edu.cn (X. Zou).

https://doi.org/10.1016/j.cclet.2022.05.050
1001-8417/

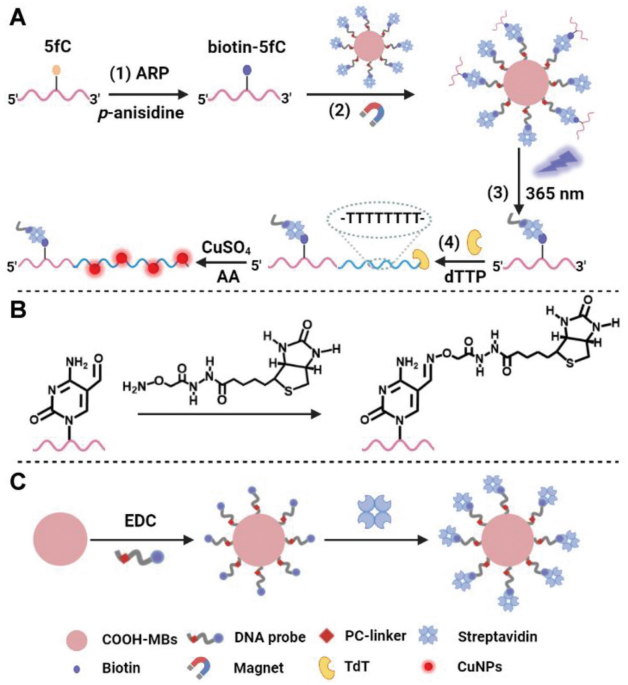

Fig. 1. (A) Schematic illustration of fluorescence detection of 5fC by 5fC-PTIAS assay. (B) Molecular mechanism for the biotinylation of 5fC-DNA using ARP. (C) Preparation of functionalized MBs with a DNA probe and streptavidin.

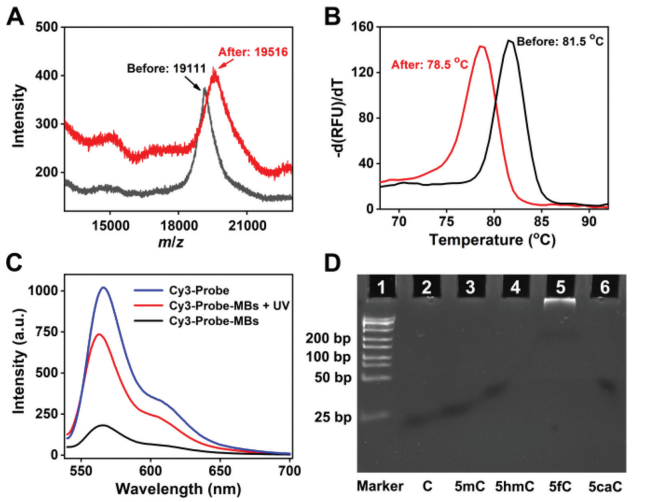

Fig. 2. (A) MALDI-TOF MS characterization of 5fC-DNA before (black line) and after (red line) biotinylation treatment. (B) Melting curves for double-stranded 5fC-DNA before (black line) and after (red line) biotinylation treatment. (C) Fluorescence intensities of supernatants of Cy3-Probe, Cy3-Probe-MBs with/without UV irradiation. (D) PAGE analysis of extended products from C-, 5mC-, 5hmC-, 5fC-, and 5caC-DNA after biotinylation, enrichment and photocleavage processes.

pull down which limits their wide application. Electrochemical methods, possessing high sensitivity by introducing electroactive molecules on 5fC, are also widely used in the detection of 5fC, but most of these methods rely heavily on complex electrode modification processes and cumbersome operations [18,19]. In comparison, the fluorescence method is cost-effective and easily-operated for the detection of most biochemical targets, which usually couples with various amplification methods for an improved sensitivity [20,21]. However, these amplification strategies, such as polymerase chain reaction (PCR) [22–24], loop-mediated isothermal amplification (LAMP) [25], and strand displacement amplification (SDA) [26], require specifically designed DNA probes and template, and most of them are only applicable for locus-specific detection of 5fC. Terminal deoxynucleotide transferase (TdT)-mediated isothermal amplification is template free and sequence independent. By coupling with magnetic enrichment, its sensitivity can be further enhanced [27], but the direct amplification of the bound target on beads may be affected by steric hindrance, restricting the amplification efficiency. The elution of targets from beads may solve this problem; however, the conventional elution method suffers from the over dilution of targets and chemical contaminations from buffer [28].

Hence, we developed a photo-elutable and template-free isothermal amplification strategy for the sensitive detection of 5fC in genomic DNA based on 5fC-specific biotinylation, enrichment, photocleavage, and TdT-assisted fluorescence signal amplification, which is termed 5fC-PTIAS. As schematically illustrated in Fig. 1A, 5fC-PTIAS assay comprises four steps: (1) Biotinylation of 5fC (biotin-5fC) through aldehyde reactive probe (ARP; *O*-(biotinylcarbazoylmethyl)hydroxylamine) in the presence of *p*-anisidine [12]. The molecular mechanism is shown in Fig. 1B, in which the oxime bond is formed by nucleophilic addition reaction between aldehyde group of 5fC and amino group of hydroxylamine. (2) Enrichment of biotinylated 5fC by the functionalized MBs, where a 3′ amino-terminated DNA probe is specially designed and conjugated on the surface of carboxyl-modified MBs *via* 1-ethyl-3-[3-dimethylaminopropyl]carbodiimide hydrochloride (EDC) activation. Besides the biotin modification at its 5′-end for streptavidin functionalization, this probe has an internal PC-linker [29] embedded for the subsequent photoelution of the captured 5fC (Fig. 1C). (3) Photocleavage. The photocleavable linker conjugated between the beads and streptavidin allows the elution of the bound 5fC-containing DNA (5fC-DNA) from MBs in one step by UV irradiation. (4) Isothermal amplification mediated by TdT to form a long poly(T) tail from the 3′-OH end of the eluted 5fC-DNA in the presence of 2′-deoxythymidine-5′-triphosphate (dTTP), resulting in the generation of fluorescent copper nanoparticles (CuNPs) [30] with the addition of $CuSO_4$ and ascorbic acid (AA). In this approach, by taking advantages of the highly specific and efficient chemolabeling process, only 5fC can be labeled with biotin group, instead of other cytosine derivatives such as 5mC, 5hmC and 5-carboxylcytosine (5caC), ensuring the high selectivity of the method. Further introducing the one-step photoelution can avoid contaminations from elution solutions, detergent, and the nonspecifically bound DNA to the beads that can not be released, leading to the minimal nonspecific background. Moreover, compared with the bound 5fC-DNA, the eluted 5fC-DNA can be sufficiently elongated without steric hindrance, generating large numbers of fluorescent CuNPs while eliminating the background noise from the light scattered by MBs. Consequently, highly sensitive and selective quantification of genomic 5fC content can be realized in different tissues with ordinary instrument due to the achievement of a high signal-to-noise ratio in this 5fC-PTIAS assay.

The successful implementation of the proposed 5fC-PTIAS assay relies on the efficient labeling of 5fC with biotin. Therefore, a 62-nt P53 promoter bearing one 5fC site as the DNA model was chosen to verify the labeling feasibility, and the sequence is listed in Table S1 (Supporting information). The generation of biotinylated 5fC-DNA was first proved by the matrix-assisted lasers desorption/ionization time-of-flight mass spectrometry (MALDI-TOF MS). The mass-to-charge ratio (m/z) of 5fC-DNA changed from 19,111 (calculated 19,093) to 19,516 (calculated 19,520) after biotinylation (Fig. 2A). Meanwhile, the melting temperature (T_m) of the double-stranded 5fC-DNA was significantly reduced by 3 °C after biotinylation step (Fig. 2B). After the biotinylation step, the product was

incubated with streptavidin, and then analyzed by polyacrylamide gel electrophoresis (PAGE). The binding of the biotinylated 5fC-DNA with streptavidin resulted in a much slower-migrating band compared to the untreated 5fC-DNA, which confirmed the successful biotinylation of 5fC-DNA (Fig. S1 in Supporting information). Based on the grayscale intensity of electrophoretic bands, the labeling efficiency was calculated as 93.5%. These results suggest that 5fC was successfully biotinylated by ARP with a high efficiency.

Before the enrichment of the biotinylated 5fC-DNA, MBs were functionalized with a DNA probe and streptavidin, forming SA-Probe-MBs conjugates, which were characterized by zeta potentials, Fourier transform infrared (FT-IR), and dynamic light scattering (DLS). After conjugated with 3′ amino-terminated DNA *via* EDC activation, the surface charge of carboxyl-modified MBs changed from −29.5mV to −16.9 mV (Fig. S2 in Supporting information), which was consistent with the previous report [31] and proved the successful construction of probe-MBs conjugates. Moreover, in the FT-IR spectrum, the peak at 1637 cm^{-1} (C=O stretching vibration) shifted to a lower frequency (1624 cm^{-1}) after DNA probe was conjugated onto the surface of MBs due to the conversion of carboxyl to amide linkage (Fig. S3 in Supporting information) [32]. After streptavidin was added, the hydrated particle size of MBs increased significantly (Fig. S4 in Supporting information), indicating the successful construction of SA-Probe-MBs conjugates. To assess the cleavage efficiency of the PC-linker under UV irradiation, the 5′ biotin labeling of DNA probe was replaced with 5′ Cy3 fluorescent group (Cy3-Probe), and the Cy3-Probe conjugated beads (Cy3-Probe-MBs) were used as a model system. As shown in Fig. 2C, the fluorescence intensity of Cy3 in supernatant decreased from 1021 to only 106 after conjugating Cy3-Probe on MBs. The loading efficiency was calculated as high as 84.8% according to the standard curve (Fig. S5 in Supporting information), which can guarantee the adequate streptavidin labeling and the high efficiency of subsequent 5fC enrichment. Meanwhile, after Cy3-Probe-MBs were irradiated with 365 nm UV light at a power density of 2.5 mW/cm^2 for 8 min, the fluorescence intensity of supernatant was recovered to 736, which was equal to 80.2% of free Cy3-Probe. Therefore, the release efficiency was calculated as 95.5% (80.2% ÷ 84.8% × 100%), indicating a high photocleavage efficiency of probes from MBs. Moreover, Fig. S6 (Supporting information) showed a rapid cleavage of the linker within 8 min, and after 8 min there were no further significant changes in the fluorescence intensity. Thus, a fixed irradiation time of 8 min was used in our system.

Next, the ability of TdT to elongate the 62-nt DNA model was verified by PAGE analysis (Fig. S7 in Supporting information). The original DNA model was obviously elongated after 30 min of enzymatic polymerization, and further elongated with up to thousands of thymine after 120 min. Moreover, the TdT-mediated poly(T)-templated CuNPs were also characterized by fluorescence spectrum, which exhibited an intense red fluorescence emission centered at 625 nm with excitation wavelength of 350 nm (Fig. S8 in Supporting information). The fluorescence intensities of CuNPs generated under different conditions were investigated, such as different concentrations of TdT, $CuSO_4$ and AA, and a different synthesis time of CuNPs (Figs. S9–S12 in Supporting information). The optimal conditions were obtained with 0.33 U/μL TdT, 300 μmol/L $CuSO_4$, and 6 mmol/L AA, when the enzymatic polymerization proceeded for 120 min followed by 5 min for CuNPs synthesis.

The TdT-catalyzed elongation of the photoeluted 5fC-DNA model was also investigated by PAGE analysis after biotinylation, enrichment and photocleavage steps (Fig. 2D). There was no obvious band in lanes of unmodified DNA model (C-DNA, lane 2), 5mC-DNA (lane 3), 5hmC-DNA (lane 4), and 5caC-DNA (lane 6). In contrast, a clear band was observed at the top of lane 5, suggesting that only biotinylated 5fC-DNA can be enriched, photoeluted and

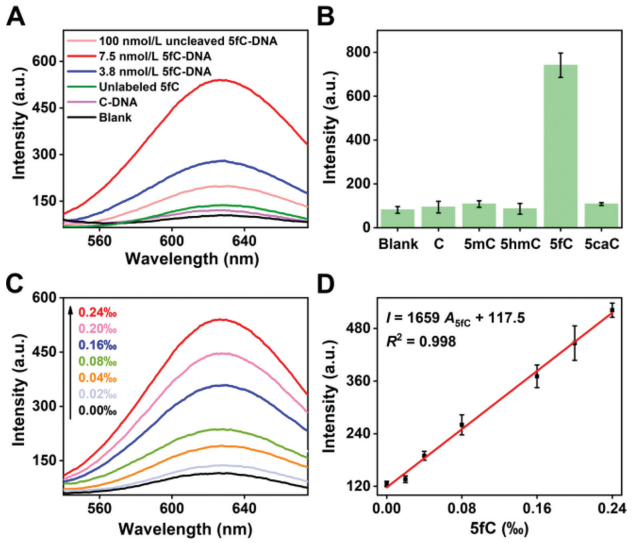

Fig. 3. (A) Fluorescence responses of 5fC-PTIAS assay to different samples. (B) Histogram of fluorescence intensities in response to 10 nmol/L C-, 5mC-, 5hmC-, 5fC-, and 5caC-DNA. (C) Fluorescence responses of 5fC-PTIAS assay to different 5fC levels in DNA models. (D) Linear plots of fluorescence intensities versus 5fC levels in DNA models.

prolonged with a long sequence of poly(T) tail. We further measured the fluorescence intensity of generated CuNPs with different samples (Fig. 3A). When Tris-EDTA (TE) buffer (10 mmol/L Tris-HCl, 1 mmol/L EDTA, pH 8.0) was analyzed as blank by this 5fC-PTIAS method, only a weak fluorescence response was obtained, indicating that the photocleaved DNA probe can hardly be prolonged by TdT in the absence of 5fC-DNA target. When 7.5 nmol/L C-DNA (as control) and unlabeled 5fC were analyzed, the fluorescence intensity slightly increased, exhibiting a low nonspecific background due to the separation ability of MBs and the introduced photoelution process. In comparison, the fluorescence intensity significantly increased with 3.8 nmol/L biotinylated 5fC-DNA, and further increased when the concentration of biotinylated 5fC-DNA increased to 7.5 nmol/L, revealing that this assay can successfully realize the determination of the biotinylated 5fC. Notably, without UV irradiation, the fluorescence intensity of 100 nmol/L uncleaved 5fC-DNA was even weaker than that of 3.8 nmol/L photocleaved 5fC-DNA, manifesting that it is necessary to introduce the photoelution process to achieve a much higher efficiency of signal amplification.

Owing to the high structure similarity among different cytosine derivatives, it is necessary to confirm whether the other derivatives interfere with the detection of 5fC-DNA. Therefore, DNA models containing different cytosine derivatives were analyzed with the same concentration of 10 nmol/L. As illustrated in Fig. 3B, only 5fC-DNA can be specifically captured, photoeluted and amplified, resulting in a significant increase in fluorescence intensity. On the contrary, the fluorescence signals of C-, 5mC-, 5hmC-, and 5caC-DNA were almost the same as that of blank. The improved resistance against interference from other cytosine derivatives can be attributed to 5fC-specific biotinylation and photoelution treatments, getting rid of other unlabeled or nonspecifically bound DNA.

To investigate the quantitative performance toward 5fC, the 5fC-DNA was first mixed in the specified proportion with C-DNA after biotinylation step, making the detectable 5fC level as 0.02‰, 0.04‰, 0.08‰, 0.16‰, 0.20‰ and 0.24‰ in DNA, and then subjected to the enrichment, photocleavage, and amplification reactions. As shown in Fig. 3C, the fluorescence intensity increased with the increasing 5fC level. It was clear that the fluorescence

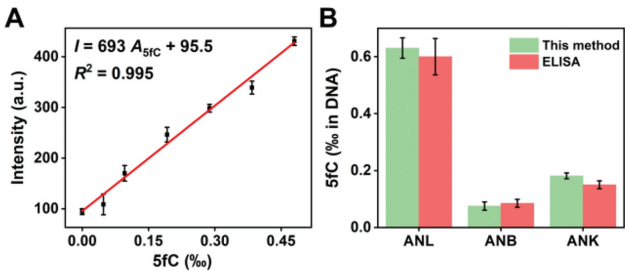

Fig. 4. (A) Linear plots of fluorescence intensities versus genomic 5fC levels in newborn mouse brain. (B) Detection of 5fC in genomic DNA extracted from different mouse tissues by this method and the ELISA kit.

intensity (I) obtained at 625 nm emission wavelength exhibited a good linear relationship with the 5fC level (A_{5fC}) in the range of 0.02‰ to 0.24‰ (Fig. 3D). The linear regression equation was $I = 1659A_{5fC} + 117.5$, with a correlation coefficient (R^2) of 0.998, and a limit of detection (LOD) of 0.01‰ in DNA (S/N = 3). Therefore, this proposed strategy had a satisfactory linear range and comparable LOD [33]. All these results suggest that the proposed 5fC-PTIAS assay has high sensitivity and selectivity, holding a great promise in target 5fC-DNA determination in real samples.

The reliability and reproducibility of the approach was evaluated through recovery experiments by spiking different levels of 5fC (0.04‰, 0.06‰, and 0.10‰) into the artificially prepared DNA sample containing 0.02‰ 5fC. As listed in Table S2 (Supporting information), the measured recovery of 5fC-DNA was in the range of 95.3%−103.0% with small relative standard deviations (RSDs) in the range of 1.8%−8.4%, suggesting an acceptable accuracy and reproducibility.

The proposed assay was further utilized to detect 5fC in genomic DNA. It has been reported that 5fC is rich in newborn mouse brain [34], thus, the genomic DNA extracted from newborn mouse brain was used as a model for the quantitative standard curve of biological samples. The extracted genomic DNA was ultrasonically fragmented to 200–250 bp in order to keep the reaction condition consistent with DNA model (Fig. S13 in Supporting information). Firstly, the genomic 5fC level in newborn mouse brain was quantified as 0.48‰ in DNA using a commercial 5fC-DNA quantification kit and served as a standard sample for calibration curve. Secondly, the genomic DNA fragments were biotinylated in the same way as 5fC-DNA model and mixed with the untreated genomic DNA fragments in diverse proportions. The mixed DNA samples were then subjected to the enrichment, photocleavage, and amplification reactions. As shown in Fig. 4A, the fluorescence intensity had a linear relationship with genomic 5fC levels in the range of 0.048‰−0.48‰ in DNA, and a linear regression equation is $I = 693A_{5fC} + 95.5$ ($R^2 = 0.995$), with a LOD of 0.025‰ in DNA (S/N = 3). Interestingly, the linear range covers the genomic 5fC level in most tissues or cells [12], encouraging us to investigate the feasibility of the proposed 5fC-PTIAS assay for detecting 5fC levels in genomic DNA from various biological samples.

According to previous researches, the global level of 5fC was tissue-specific, and showed dynamic changes with differentiation, aging and the occurrence of various diseases [34]. In this research, based on the obtained calibration curve genomic DNA sample, the genomic 5fC levels of adult nude mouse brain (ANB), kidney (ANK), and liver (ANL) were quantified as 0.075‰, 0.181‰, and 0.631‰ in DNA, respectively, which were highly consistent with those measured by an ELISA kit (Fig. 4B). Compared with the ELISA kit based on 5fC antibodies that typically show CpG-density-related bias [6], our 5fC-PTIAS strategy provides considerable improvement with smaller errors due to a more comprehensive and accurate labeling of 5fC, which can determine 5fC in real samples sensitively and accurately by further coupling the photo-elutable and template-free amplification reaction. The above data showed the inhomogeneous distribution of 5fC among different tissues, and moreover, the 5fC level of newborn mouse brain (0.48‰) was much higher than that of adult mouse brain (0.075‰). These results suggest that 5fC plays an important role in the development of mammalian organs especially the brain tissue, which may be closely related to the regulation of DNA demethylation.

In conclusion, an efficient 5fC-PTIAS strategy is constructed for the sensitive fluorescence detection of 5fC in genomic DNA. This isothermal amplification-based strategy is bisulfite-free, PCR-free and template-free, and can get rid of severe DNA degradation, different temperature setting and specifically designed DNA probes. Moreover, compared with the previous report that directly amplified the bound 5hmC-DNA target on beads [27], our photocleavable 5fC-PTIAS strategy specially initiates the amplification on the photoeluted 5fC-DNA without steric hindrance, showing a high signal-to-noise ratio and holding great promise in detecting 5fC with much lower level in real samples. Inspiringly, this 5fC-PTIAS assay with a detection limit of 0.025‰ in DNA is capable of quantifying genomic 5fC content in various mammal tissues with easy operation and handy equipment in the laboratory. For analysis of rare clinical samples, the sample input of the proposed method should be further lowered by well designing the amplification reaction with higher kinetics in the future.

Declaration of competing interest

The authors report no declarations of interest.

Acknowledgments

This work was supported by the Scientific Technology Project of Shenzhen City (Nos. JCYJ20200109142410170 and JCYJ20210324124003008), the National Natural Science Foundation of China (No. 21974153), the Scientific Technology Project of Guangzhou City (No. 202103000003), the Guangdong Natural Science Foundation (No. 2019A1515010587), and the Guangdong Science and Technology Plan Project (No. 2020B1212060077).

Supplementary materials

Supplementary material associated with this article can be found, in the online version, at doi:10.1016/j.cclet.2022.05.050.

References

[1] S. Ito, L. Shen, Q. Dai, et al., Science 333 (2011) 1300–1303.
[2] L. Zhang, W. Chen, L. Iyer, et al., J. Am. Chem. Soc. 136 (2014) 4801–4804.
[3] T. Pfaffeneder, B. Hackner, M. Truß, et al., Angew. Chem. Int. Ed. 123 (2011) 7146–7150.
[4] M. Iurlaro, G. McInroy, H. Burgess, et al., Genome Biol. 17 (2016) 141.
[5] A. Inoue, L. Shen, Q. Dai, et al., Cell Res. 21 (2011) 1670–1676.
[6] X. Wu, Y. Zhang, Nat. Rev. Genet. 18 (2017) 517–534.
[7] S. Ji, H. Shao, Q. Han, et al., Angew. Chem. Int. Ed. 56 (2017) 14130–14134.
[8] E. Raiber, G. Portella, S. Cuesta, et al., Nat. Chem. 10 (2018) 1258–1266.
[9] F. Li, Y. Zhang, J. Bai, et al., J. Am. Chem. Soc. 139 (2017) 10617–10620.
[10] T. Storebjerg, S. Strand, S. Høyer, et al., Clin. Epigenetics 10 (2018) 105.
[11] J. Liu, J. Jiang, J. Mo, et al., Hepatology 69 (2019) 196–208.
[12] E. Raiber, D. Beraldi, G. Ficz, et al., Genome Biol. 13 (2012) R69.
[13] C. Song, K. Szulwach, Q. Dai, et al., Cell 153 (2013) 678–691.
[14] F. Neri, D. Incarnato, A. Krepelova, et al., Nat. Protoc. 11 (2016) 1191–1205.
[15] M. Booth, G. Marsico, M. Bachman, et al., Nat. Chem. 6 (2014) 435–440.
[16] H. Hong, Y. Wang, Anal. Chem. 79 (2007) 322–326.
[17] M. Lan, B. Yuan, Y. Feng, Chin. Chem. Lett. 30 (2019) 1–6.
[18] Q. Wang, H. Yin, Y. Zhou, et al., Sens. Actuators B: Chem. 341 (2021) 130019.
[19] F. Li, H. Yi, Y. Chen, et al., J. Colloid Interface Sci. 561 (2020) 348–357.
[20] Y. Xu, Y. Zhang, H. Yang, et al., Chin. Chem. Lett. 33 (2022) 968–972.
[21] Q. Wang, J. Ding, J. Xiong, et al., Chin. Chem. Lett. 32 (2021) 3426–3430.
[22] Y. Wang, C. Liu, X. Zhang, et al., Chem. Sci. 9 (2018) 3723–3728.
[23] S. Wang, Y. Song, L. Wei, et al., J. Am. Chem. Soc. 139 (2017) 16903–16912.
[24] J. Liu, W. Yang, X. Zhang, et al., Chem. Commun. 57 (2021) 13796–13798.

[25] Z. Zhang, D. Yang, W. Tian, et al., Anal. Chem. 92 (2020) 3477–3482.
[26] D. Chen, Y. Wang, M. Mo, et al., Nucleic Acids Res. 47 (2019) e119.
[27] C. Li, Y. Dong, X. Zou, et al., Anal. Chem. 93 (2021) 1939–1943.
[28] S. Cho, S. Lee, W. Chung, et al., Electrophoresis 25 (2004) 3730–3739.
[29] Z. Qing, X. He, D. He, et al., Angew. Chem. Int. Ed. 52 (2013) 9719–9722.
[30] J. Chen, M. Wang, Y. Bao, et al., ACS Appl. Bio. Mater. 4 (2021) 5669–5677.
[31] W. Tang, R. Mi, L. Wang, et al., Sens. Actuators B: Chem. 340 (2021) 129969.
[32] J. Jang, H. Lim, Microchem. J. 94 (2010) 148–158.
[33] M. Gieß, Á. Muñoz-López, B. Buchmuller, G. Kubik, D. Summerer, J. Am. Chem. Soc. 141 (2019) 9453–9457.
[34] M. Bachman, S. Uribe-Lewis, X. Yang, et al., Nat. Chem. Biol. 11 (2015) 555–557.